Resonant Raman scattering study of Ar^+ ion-implanted AlGaN

2005 J. Phys.: Condens. Matter 17 1995

(http://iopscience.iop.org/0953-8984/17/12/021)

INSTITUTE OF PHYSICS PUBLISHING JOURNAL OF PHYSICS: CONDENSED MATTER

J. Phys.: Condens. Matter **17** (2005) 1995–2002 doi:10.1088/0953-8984/17/12/021

Resonant Raman scattering study of Ar^+ ion-implanted AlGaN

B Boudart[1], Y Guhel[1], J C Pesant[2], P Dhamelincourt[3] and M A Poisson[4]

[1] Laboratoire Universitaire des Sciences Appliquées de Cherbourg, EA 2607, Site Universitaire, BP 78, 50130 Cherbourg-Octeville, France
[2] Institut d'Electronique de Microélectronique et de Nanotechnologie, UMR-CNRS 8520, Département Hyperfréquences et Semiconducteurs, Université des Sciences et Technologies de Lille, 59652 Villeneuve d'Ascq Cedex, France
[3] Laboratoire de Spectrochimie Infrarouge et Raman, UMR-CNRS 8516, Centre d'Etudes et de Recherches Lasers et Applications, Université des Sciences et Technologies de Lille, 59655 Villeneuve d'Ascq Cedex, France
[4] THALES, Laboratoire Central de Recherches, Domaine de Corbeville, 91404 Orsay Cedex, France

E-mail: bertrand.boudart@chbg.unicaen.fr

Received 22 October 2004, in final form 16 February 2005
Published 11 March 2005
Online at stacks.iop.org/JPhysCM/17/1995

Abstract

160 keV Ar^+ ions were homogeneously implanted in AlGaN at room temperature for device isolation purposes. Resonance Raman spectroscopy and DC electrical measurements were used to monitor the structural and electrical changes of the non-annealed and annealed implanted AlGaN samples with a dose ranging from 3.4×10^{12} to 1×10^{16} ions cm^{-2}. The annealing was carried out at 900 °C for 40 s, these conditions being necessary to achieve good Ohmic contacts. On increasing the implantation dose from 3.4×10^{12} to 3.4×10^{14} ions cm^{-2}, an increase in the electrical isolation and a decrease in the photoluminescence (PL) were observed. For the highest dose, the implanted layer becomes conductive, probably due to a hopping mechanism. After annealing, the implanted samples become conductive and the PL reappears or increases as compared to the non-annealed samples using the same implantation doses. Then, it is possible to obtain good device electrical isolation by implanting ions with a 3.4×10^{14} cm^{-2} dose subsequently to the annealing process necessary to achieve Ohmic contacts.

1. Introduction

The AlGaN–GaN heterostructure material system holds a strong interest for optical [1], high power electronic [2] and high temperature [3, 4] applications due to its superior material properties. The conventional AlGaN–GaN heterostructure field effect transistor (HFET)

structure consists of a nucleation layer grown on a sapphire or a silicon carbide substrate, followed by intentionally non-doped GaN and finally by an AlGaN top barrier layer. Sometimes this AlGaN layer is n-type doped to improve the Ohmic contact quality. During the fabrication of HFETs, the making of the device active area is realized by mesa etching using dry or wet processes or, even, by implant isolation [5]. The most important advantage of this technique is maintaining a planar wafer surface suitable for device processing. Electrical isolation of GaN by H, He, N, F, Ar, Mg and Zn ion implantation has been previously reported [6–12]. Implant isolations were achieved in AlGaN using Zn, Mg/C and P/He ions [12–14]. Generally, the ion implantation technological step needs a thermal annealing. Moreover, the source and drain contacts of HFETs also need a subsequent annealing operation, performed at high temperature in the case of GaN or AlGaN, to become Ohmic [15].

Resonant Raman scattering provides a powerful tool for studying the vibrational properties of the structures. Under resonant conditions, the Raman spectra of hexagonal III–V nitrides are dominated by Frölich scattering associated with the longitudinal polar optical phonons. This technique is very sensitive due to the strong polarity of the bonds in these compounds. Multi-phonon scattering up to the sixth order has been observed in the case of GaN [10].

In the present paper, we report on resonant Raman spectroscopic and electrical studies made on AlGaN samples, which were implanted with Ar^+ ions for device isolation purposes. This atomic species was chosen owing to its electrically neutral character but also due to the good results obtained previously for GaN [10]. The aim of these original studies was to determine, on a one hand, whether it is possible to isolate electrically two devices on AlGaN/GaN by implanting Ar^+ ions; to answer this question, the influence of the implantation dose on the device isolation was studied. On the other hand, in the case of a positive answer, the aim was to establish the order of the technological steps which should be made between ion implantation and Ohmic contact annealing. That is the reason that these analyses were performed on both post-implant non-annealed and annealed samples.

2. Experimental details

2.1. Sample processing

The AlGaN–GaN heterostructure was grown by a metal–organic chemical vapour deposition process on a *c*-plane sapphire substrate. The epitaxial growth began with a 25 nm GaN nucleation layer, followed by a 1.2 μm thick intentionally non-doped GaN layer, followed by a 200 nm thick n-type $Al_{0.15}Ga_{0.85}N$ barrier layer. The doping level of this barrier layer was 3×10^{17} cm^{-3} as determined at room temperature by Hall measurements. The Al content was measured by means of x-ray diffraction. Device fabrication started with the Ohmic contact formation. Ti/Al/Ni/Au (15/220/40/50 nm) was evaporated and then alloyed at 900 °C for 40 s to achieve good Ohmic contacts, allowing us to perform the isolation electrical measurements by the four-probe method. The distance between two Ohmic contacts was 5 μm. After this technological step, a sample was cut from the wafer to serve as a reference for the study. All the samples used in this study were pieces cut from the same wafer. The samples were then put in an Eaton 3204 implanter for implanting at room temperature the AlGaN layer with 160 keV Ar^+ ions using fluences from 3.4×10^{12} to 1×10^{16} cm^{-2}. During the implantation process, the Ohmic contacts were protected with a photoresist coating. After the implantation process, this coating was removed in an acetone bath and the samples were both electrically and Raman analysed. Then, a post-implant annealing was realized in the same conditions as for forming the Ohmic contacts in order to allow a comparison with the non-post-implant annealed samples.

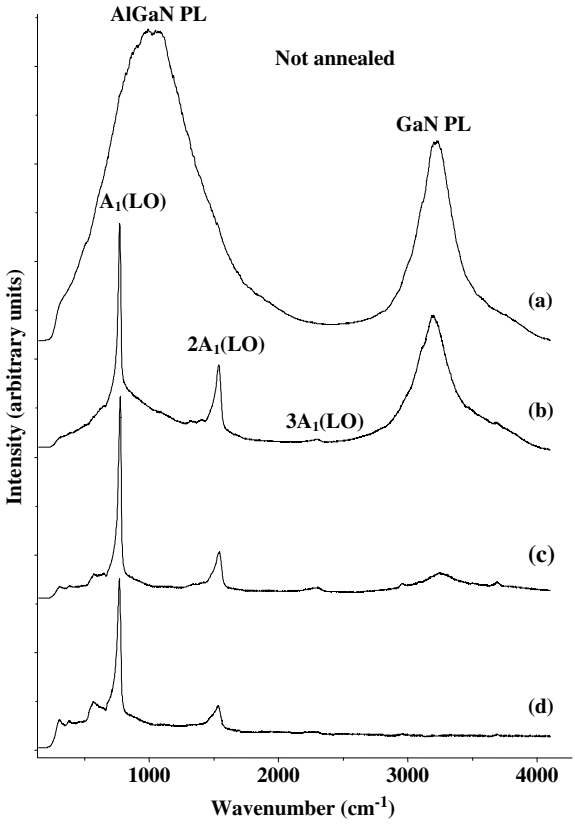

Figure 1. (a) Raman spectrum of the reference sample. The implanted materials were obtained after 160 keV Ar^+ ion implantation at doses of (b) 3.4×10^{12}, (c) 3.4×10^{13} and (d) 3.4×10^{14} cm^{-2}.

2.2. Raman spectroscopy

Raman spectra were recorded at room temperature in a back-scattering configuration from the growth surface with the laser beam propagating parallel to the *c* axis. A He–Cd laser ($\lambda = 325$ nm) was used as the excitation source. The energy of the exciting radiation is far higher than that of the AlGaN gap one, allowing photoluminescence (PL) to be measured. The incident light power was less than 1 mW on the sample surface. All the measurements were performed at the Jobin-Yvon company (Villeneuve d'Ascq—France) using a UV LABRAM Raman microspectrometer. A 100× UV objective was used, giving a spot size smaller than 1 μm on the sample surface. A 100 μm entrance slit opening was used, giving a 8.4 cm^{-1} spectral resolution.

3. Results and discussion

In figure 1, the Raman spectra of the samples before and after implantation without post-annealing are shown. The Raman spectrum of the reference sample exhibits only two strong PL features, located at 1010 and 3220 cm^{-1}, which are attributed to band to band recombination of AlGaN and GaN materials, respectively (see figure 1(a)). The gap energy of the AlGaN material depends on the Al content [16–18]. Then, it was possible to estimate the Al content of the AlGaN layer to be 15% from the PL energy. This value is consistent with the results

obtained from x-ray diffraction. Owing to these strong PL emissions, the Raman lines were not observed for the reference sample.

After ion implantation of the AlGaN top layer with a 3.4×10^{12} cm^{-2} dose, the PL emission due to AlGaN disappeared and the PL emission due to GaN decreased (see figure 1(b)). This PL emission is very sensitive to both the presence of extended defects and the presence of point defects such as impurities, vacancies and interstices which may form deep levels in the band gap, thus serving as non-radiative pathways for carrier recombinations [19]. At the same time, owing to the PL decrease, the A_1(LO) Raman band due to the AlGaN material becomes visible at 768 cm^{-1} and two additional Raman bands were observed at approximately 1534 and 2300 cm^{-1}. These last bands were assigned to the A_1(LO) multi-phonon scattering up to the third order. The observation of these multi-phonon structures is possible in resonant Raman conditions and proves that the crystalline quality of the implanted sample remains fairly good. The observation of these Raman bands is consistent with the Raman selection rules for semiconductors having a wurtzite crystal structure [20].

On increasing the implantation dose from 3.4×10^{12} to 3.4×10^{14} cm^{-2}, the PL intensity due to the GaN material strongly decreased and disappeared (see figures 1(b)–(d)). At the same time, the intensity of the different Raman bands decreased. After ion implantation, the wavenumber and the width at half-maximum of the A_1(LO) Raman band remained at 768 ± 1 cm^{-1} and 29 ± 3 cm^{-1}, respectively. However, it was not possible to compare these values to those obtained for the reference sample due to the strong PL emission masking the Raman spectrum as mentioned before. Nevertheless, Hayashi *et al* [21] have reported for the first time the Raman spectra of AlGaN epitaxial layers with a low Al content. This study was completed later for all Al contents ranging between 0 and 100% [22–24]. These studies allow us to obtain a relation linking the A_1(LO) Raman band wavenumber to the Al content. Then, in our case for a 15% Al content, it was possible to predict that the wavenumber of the A_1(LO) Raman band should be 771 cm^{-1}. By comparing this value with the one obtained for implanted samples we can conclude that the 3 cm^{-1} observed shift can probably be attributed to the implantation-induced extensive stress.

In figures 1(c) and (d), additional broad bands located below 700 cm^{-1} are clearly observed in the Raman spectra. This phenomenon was also observed using the same Raman configuration for GaN implanted with Ar^+, or Mg^+, or P^+, or C^+, or Ca^+ ions at high dose [10, 11, 25]. These broad bands could be attributed to disorder-activated Raman modes, except that, in our case, the band appearing at about 300 cm^{-1} is an artefact due to the cut-off of the dielectric filter used to suppress the exciting line. In fact, the high implantation dose used here induces high crystalline damages so the wavevector conservation rules for the Raman scattering break down and the phonons from the entire Brillouin zone are observed in the Raman spectrum. Hence, the Raman spectrum reflects the total phonon density of states [26]. This is confirmed by the experiments performed by transmission electron microscopy on the Ar^+ ion-implanted GaN samples which indicate an amorphization of the implanted material [27]. The Raman spectrum of the sample implanted with a high ion dose (1×10^{16} cm^{-2}) was not shown in figure 1 because only the noise was observed, indicating that the damage caused by this high ion dose was too important for observing the Raman signal.

Electrical resistances were measured for as-implanted samples and also for samples which were subsequently annealed at 900 °C for 40 s. The experimental results are presented in figure 2. These resistances were measured, between two Ohmic contacts separated from 5 μm, for the different fluences used. The resistance value obtained for the non-implanted sample, which serves as a reference, is also shown for comparison. After implantation, the electrical resistance increased as a function of the fluence and reached the upper detection limit of the measurement apparatus for the 3.4×10^{14} cm^{-2} fluence. Thus, for the highest fluence

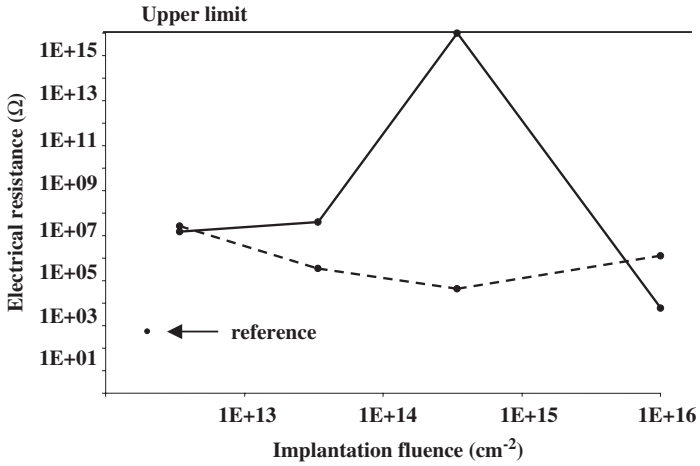

Figure 2. Evolution of the electrical resistances, versus the implantation fluence, of as-implanted samples (solid line) and samples after subsequent annealing at 900 °C for 40 s (dashed line). The electrical resistance value of a non-implanted (reference) sample is shown for comparison.

used, the sample becomes conductive, probably because of a hopping mechanism attributed to a high defect density as previously reported [28]. After a subsequent annealing at 900 °C for 40 s, all the samples become conductive. It is also worth noting that the electrical resistance value is always higher after implantation than before, indicating clearly the influence of the implantation.

In figure 3, the Raman spectra of both the reference and the implanted samples after a subsequent post-annealing at 900 °C for 40 s are shown. In comparison to the spectra shown in figure 1, several differences can be noted. After annealing, the PL intensity attributed to GaN has clearly increased compared with that observed for the non-annealed samples implanted with the same doses up to 3.4×10^{13} cm^{-2}. This can be seen by comparing the intensity of the PL emission with that of the Raman bands. This phenomenon has also been observed for Mg/P-implanted GaN after an annealing performed above 1200 °C [29] and also for Mg- or Ar-implanted GaN after a subsequent annealing performed at 900 °C [10, 11]. For the lowest fluence (3.4×10^{12} cm^{-2}), the PL intensity attributed to AlGaN becomes apparent and, consequently, the Raman bands were hardly observable. For a higher fluence (3.4×10^{14} cm^{-2}), the third-order multi-phonon Raman structures become apparent after annealing the samples (see figure 3(d)). Finally, for the highest fluence used, the implanted and subsequently annealed material shows only broad bands which were attributed to disorder-activated Raman modes as previously observed in the case of GaN [10, 11]. In that case, where the wavenumber of the highest band located at 755 cm^{-1} could be attributed to A_1(LO), the sample has not recovered a good crystalline quality, opposite to the results obtained previously for Ar^+ ion-implanted GaN [10]. After the post-implantation annealing, the width at half-maximum of the A_1(LO) band decreases to 20 ± 3 cm^{-1} whatever the ion dose used, except for the highest dose where the width at half-maximum has the double value. Moreover, for the lowest ion dose (3.4×10^{13} cm^{-2}), the AlGaN A_1(LO) band wavenumber shifted up to 770 ± 1 cm^{-1}, close to the 771 cm^{-1} reference value obtained for a 15% Al content. This proves that the annealing improves the crystalline quality of the samples.

Thus, opposite to the results obtained previously for the Ar^+ or Mg^+ ion-implanted GaN samples [10, 11], our finding is that there is only one possibility for isolating two different devices by using an Ar^+ ion implantation. In this case, a 3.4×10^{14} cm^{-2} fluence is needed

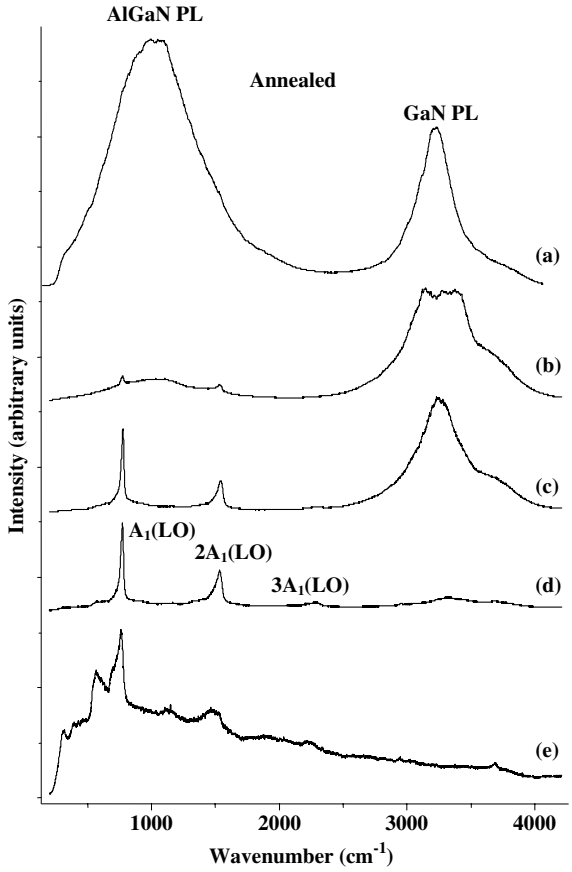

Figure 3. (a) Raman spectrum of the reference sample. The implanted materials were obtained after 160 keV Ar^+ ion implantation at doses of (b) 3.4×10^{12}, (c) 3.4×10^{13}, (d) 3.4×10^{14} and (e) 1×10^{16} cm^{-2} and after subsequent annealing at 900 °C for 40 s.

for the implantation which has to be performed after the annealing process in order to achieve good Ohmic contacts. Moreover, after this implantation, no further annealing of the implanted material is needed. In conclusion: if the implantation fluence is not high enough, the samples remain conductive but, if the implantation fluence is too high, the samples again become conductive probably because of a hopping mechanism attributable to a high defect density.

In the strained AlGaN/GaN heterostructures, the electron concentration is very sensitive to a piezoelectric effect [30]. Then, in GaN, the source to drain current is essentially located at the interface between AlGaN and GaN. For a fluence value allowing a good electrical isolation, the PL features attributed to AlGaN and GaN disappeared from the Raman spectrum. Thus, the defect density was so high that we did not observe the signal from GaN, indicating that this material is probably damaged down to the interface between AlGaN and GaN. Moreover, as seen in figure 1, the AlGaN layer is extensively stressed after the implantation step, modifying the piezoelectric field. All these observations can explain why the electrical isolation is possible. After a subsequent annealing, an atomic rearrangement of the structure is observed causing the extensive stress of the AlGaN layer to be relaxed. Thus, we suppose that the crystalline quality of the interface between AlGaN and GaN materials is improved, explaining why the samples become conductive.

4. Conclusion

The influence of Ar^+ implantation fluence on the electrical isolation properties of the AlGaN material with a 15% Al content was studied by means of DC electrical measurements and resonant Raman spectroscopy. These studies allowed us to show that it is possible to isolate electrically two different transistors by using a 3.4×10^{14} cm^{-2} fluence. The annealing of the Ohmic contacts has to be performed before the ion implantation. No further post-implantation annealing is needed to ensure the electrical isolation properties.

In order to complete this work, it should be interesting to study the influence of the Al content of AlGaN on the electrical isolation properties of the Ar^+ ion-implanted material. Moreover, due to the fact that the implanted and post-annealed samples become conductive, it should also be interesting to study the thermal stability of these implanted samples.

Acknowledgments

The authors gratefully acknowledge the financial support of the DGA. The Centre d'Etudes et de Recherches Lasers et Applications (CERLA) is supported by the Ministère chargé de la Recherche, the Région Nord-Pas de Calais and the Fonds Européen de Développement Economique des Régions. This work benefited from the equipment made available at the Jobin-Yvon company (Villeneuve d'Ascq—France). The authors thank M Moreau (Jobin-Yvon) for her help in using the UV LABRAM instrument.

References

[1] Nakamura S, Mukai T and Senoh M 1994 *Appl. Phys. Lett.* **64** 1687
[2] Wu Y F, Saxler A, Moore M, Smith R P, Sheppard S, Chavarkar P M, Wisleder T, Mishra U K and Parikh P 2004 *Electron Device Lett.* **25** 117
[3] Daumiller I, Kirchner C, Kamp M, Ebeling K J and Kohn E 1999 *Electron Device Lett.* **20** 448
[4] Guhel Y, Boudart B, Hoel V, Werquin M, Gaquière C, De Jaeger J C, Poisson M A, Daumiller I and Kohn E 2002 *IEE Microw. Opt. Technol. Lett.* **34** 4
[5] Williams R 1990 *Modern GaAs Processing Methods* (Boston, MA: Artech House Publishers)
[6] Binari S C, Dietrich H B, Kelner G, Rowland L B and Doverspike K 1995 *J. Appl. Phys.* **78** 3008
[7] Pearton S J, Vartuli C B, Zolper J C, Yuan C and Stall R A 1995 *Appl. Phys. Lett.* **67** 1435
[8] Wilson R G, Vartuli C B, Abernathy C R, Pearton S J and Zavada J M 1995 *Solid-State Electron.* **38** 1329
[9] Zolper J C 1997 *J. Cryst. Growth* **178** 157
[10] Boudart B, Guhel Y, Pesant J C, Dhamelincourt P and Poisson M A 2002 *J. Raman Spectrosc.* **33** 283
[11] Boudart B, Guhel Y, Pesant J C, Dhamelincourt P and Poisson M A 2004 *J. Phys.: Condens. Matter* **16** S49
[12] Oishi T, Miura N, Suita M, Nanjo T, Abe Y, Ozeki T, Ishikawa H, Egawa T and Jimbo T 2003 *J. Appl. Phys.* **94** 1662
[13] Polyakov A Y, Shin M, Skowronski M, Wilson R G, Greve D W and Pearton S J 1997 *Solid-State Electron.* **41** 703
[14] Hanington G, Hsin Y M, Liu Q Z, Asbeck P M, Lau S S, Asif Kahn M, Yang J W and Chen Q 1998 *IEE Electron. Lett.* **34** 193
[15] Boudart B, Trassaert S, Wallart X, Pesant J C, Yaradou O, Théron D, Crosnier Y, Lahreche H and Omnes F 2000 *IEEE J. Electron. Mater.* **29** 603
[16] Stutzmann M, Ambacher O, Cros A, Brandt M S, Angerer H, Dimitrov R, Reinacher N, Metzger T, Höpler R, Brunner D, Freudenberg F, Handscuh R and Deger C 1997 *Mater. Sci. Eng.* B **50** 212
[17] Ambacher O, Dimitrov R, Lentz D, Metzger T, Rieger W and Stutzmann M 1997 *J. Cryst. Growth* **170** 335
[18] Omnes F, Marenco N, Haffouz S, Lahreche H, De Mierry P, Beaumont B, Hageman P, Monroy E, Calle F and Muñoz E 1999 *Mater. Sci. Eng.* B **59** 401
[19] Popovici G, Xu G Y, Botchkarev A, Kim W, Tang H, Salvador A and Morkoç H 1997 *J. Appl. Phys.* **82** 4020
[20] Cardona M 1982 *Light Scattering in Solids II* vol 50, ed M Cardona and G Güntherodt (Berlin: Springer) p 10
[21] Hayashi K, Itoh K, Sawaki N and Akasaki I 1991 *Solid State Commun.* **77** 115
[22] Cros A, Angerer H, Ambacher O, Stutzmann M, Höpler R and Metzger T 1997 *Solid State Commun.* **104** 35

[23] Demangeot F, Groenen J, Frandon J, Renucci M A, Briot O, Ruffenach-Clur S and Aulombard R L 1997 *MRS Int. J. Nitride Semicond. Res.* **2** 40
[24] Demangeot F, Frandon J, Renucci M A, Sands H S, Batchelder D N, Briot O and Ruffenach-Clur S 1999 *Solid State Commun.* **109** 519
[25] Limmer W, Ritter W, Sauer R, Mensching B, Liu C and Rauschenbach B 1998 *Appl. Phys. Lett.* **72** 2589
[26] Siegle H, Kaczmarczyk G, Filippidis L, Litvinchuk A P, Hoffmann A and Thomsen C 1997 *Phys. Rev.* B **55** 7000
[27] Liu C, Mensching B, Volz K and Rauschenbach B 1997 *Appl. Phys. Lett.* **71** 2313
[28] Zolper J C, Tan H H, Williams J S, Zou J, Cockayne D J H, Pearton S J, Hagerott Crawford M and Karlicek R F 1997 *Appl. Phys. Lett.* **70** 2729
[29] Kuball M, Hayes J M, Suski T, Jun J, Leszczynski M, Domagala J, Tan H H, Williams J S and Jagadish C 2000 *J. Appl. Phys.* **87** 2736
[30] Ambacher O, Smart J, Shealy J R, Weiman N G, Chu K, Murphy M, Scaff W J, Eastman L F, Dimitrov R, Wittmer L, Stutzmann M, Rieger W and Hilsenbeck J 1999 *J. Appl. Phys.* **85** 3222